BUTTERWORTH HEINEMANN

Polymer Vol. 36 No. 6, pp. 1217–1221, 1995

0032-3861/95/$10.00+0.00

Temperature distribution in poly(ethylene terephthalate) plate undergoing heat treatment. Diffusion influence and application

Ph. Lebaudy*, J. M. Saiter, J. Grenet and C. Vautier
L.E.C.A.P., Faculté des Sciences de Rouen, BP 118, 76134 Mont-Saint-Aignan Cedex, France
(Received 2 February 1994; revised 4 July 1994)

In a previous paper, a model was developed to calculate energy efficiency and temperature profiles inside a polymer plate undergoing heat treatment. This model links up the radiator characteristics and the crystalline structures together with the material i.r. absorption behaviour. Here, to validate the model, we present a comparison between numerical simulation and experimental results carried out on poly(ethylene terephthalate) plates. Examples are then given which illustrate the possible applications of the model. Finally, simulation and experimental results on the crystalline fraction distribution inside the material are presented.

(Keywords: polymer processing; temperature distribution; crystallinity)

INTRODUCTION

During plastic forming processes, the semi-finished thermoplastic products must be brought to a rubber-like state by supplying heat to them. Heating by means of infra-red radiation is a convenient and widely used method. An understanding of this heating stage generally requires knowledge of the temperature distributions inside the material. However, measurement of these temperature distributions during the actual process is impossible, both with contactless methods such as the radiation pyrometer and i.r. camera, and with contact methods such as thermocouples. Thus many unnecessary and costly production delays result from the inability to determine when the material has been thoroughly heated to the suitable stretching temperature.

Owing to these reasons, numerous computation studies of this industrial process[1–3] are available in the literature. In most of these works, the calculation of radiation transfer between solid bodies is based on the assumption of black bodies or grey bodies. The resulting solutions of these computations must be applied carefully to thermoplastics, because of the strong spectral dependence of the thermoplastic absorption characteristics. Moreover, the i.r. scattering induced by the polymeric crystalline structure is generally neglected.

In a previous paper[4], with the aim to calculate the temperature distribution inside a semicrystalline polymer plate undergoing heat treatment, we presented a model which links up the radiator characteristics and the optical properties of the polymer (absorption and scattering phenomena). In this model the temperature distribution is given by the unsteady-state heat conduction equation with two location-dependent heat sources:

$$\frac{\delta^2 T}{\delta x^2} - \frac{1}{a}\frac{\delta T}{\delta \tau} + \frac{S(x)}{k} + \frac{\Delta H_c}{aC_p}\frac{\delta \alpha(x)}{\delta \tau(x)} = 0$$

which needs the knowledge of the heat source $S(x) = \int_{\lambda_1}^{\lambda_2} S_\lambda(x)\,\mathrm{d}\lambda$, with

$$S_\lambda(x) = -\frac{\mathrm{d}\Phi_\lambda(x)}{\mathrm{d}x} = -\frac{\mathrm{d}[(I_\lambda^+ - I_\lambda^-) + \pi(L_\lambda^+ - L_\lambda^-)]}{\mathrm{d}x}$$

where I_λ^+ and I_λ^- (the collimated fluxes) and L_λ^+ and L_λ^- (the isotropic irradiances) lead to a four-flux model[5,6].

If the polymer temperature goes through the crystallization temperature range, this model takes into account the eventual modifications of the optical properties which occur during the thermal process. Indeed, it is a matter of fact that the polymer crystallization modifies the material structure and therefore the scattering parameters.

This paper deals with both experimental and theoretical applications of the model. The experimental results allow us to check the validity of the model. Theoretical results are presented for different examples which emphasize the influence of the radiator temperature, the convective parameter, the polymer structure and the scattering properties on the temperature profile inside the material. Moreover, an application to the determination of the crystalline fraction distribution inside a polymer plate is given.

*To whom correspondence should be addressed

EXPERIMENTAL

Measured data

The measured data were obtained from a poly(ethylene terephthalate) (PET) plate of 4 mm wall thickness, heated in a prototype oven equipped with bright radiators. The radiator temperature, controlled by a radiation pyrometer, is given with an uncertainty of 5°C. The temperatures inside the plate were measured using fine thermocouples placed at different distances from the surface. Their response time is 0.5 s for a temperature step of 80°C. The surface temperature was determined by means of a radiation thermometer. These measurements lead to an uncertainty on the temperature values of less than ±5°C. An electric fan gives the possibility to change the convective parameter on the material surfaces in the oven (surface heat transfer coefficient in the simulation) from 5 W m^{-2} K^{-1} (natural convection) to 200 W m^{-2} K^{-1} (forced convection).

Calculated data

In our model[4], all the thermal parameters of the oven system and the material could be changed independently. Their experimental ranges are reported in *Table 1*.

This set of parameters has been chosen to be realistic for an industrial process without any drastic conditions.

RESULTS

Influence of radiator temperature

On *Figure 1* we report computed curves of the variations of surface temperature of an amorphous polymer plate (thickness 4 mm) *versus* time, with radiator temperature (curve a: $T_r = 1500$ K; curve b: $T_r = 2000$ K) and irradiance (curves a, b: irradiance = 20 000 W m^{-2}; curve c: irradiance = 6500 W m^{-2}) as parameters. The given curves are calculated for a heating time $t = 10$ s; after this heating the plate is cooled during 10 s (convective parameter = 70 W m^{-2} K^{-1}). *Figure 2* shows the variation of temperature at the end of heating *versus* the distance from the irradiated surface. For a given irradiance (curves a and b of *Figures 1* and *2*) the better heating efficiency is obtained for low radiation temperature, but in this case the thermal gradient between both sides is high. Although these two examples are of interest for understanding the phenomenon, they are not realistic because a decrease in radiator temperature not only leads to a shift towards higher wavelengths of the emitted radiation (which enhances the energy efficiency) but also to a modification of the irradiance. The comparison of curves b and c (*Figures 1* and *2*) is better in the sense that the ratio of the irradiances is the same as that of the fourth power of the radiator temperature (Stefan–Boltzmann law).

Figure 1 also reports the experimental data. Good agreement is obtained between measured and calculated data during both heating and cooling phases. The value of the surface heat transfer parameter [70 W m^{-2} K^{-1} (forced convection)] chosen to obtain calculated curves in good agreement with experimental ones lies within usual experimental values.

Influence of material structure

Generally, to attain high radiation penetration into the depth of the polymer plate (Figure 2 in ref. 4) and therefore to obtain a uniform temperature distribution, one uses short-wave i.r. radiation (radiator temperature > 2500 K).

Table 1 Thermal parameters of the oven, and thermal and physical parameters of the material

Oven		
T_r	radiator temperature	1000 to 2500 K
R_i	radiator irradiance	50 000 to 200 000 W m^{-2}
C_0	convective parameter on the front	5 to 200 W m^{-2} K^{-1}
C_i	convective parameter on the back	5 to 200 W m^{-2} K^{-1}
T_0	ambient temperature on the front	20 to 100°C
T_i	ambient temperature on the back	20 to 100°C
t_h	heating duration	5 to 50 s
t_t	total simulated time	5 to 200 s
Material		
a	thermal diffusivity	refs 7 and 8
A_λ	spectral absorptivity	Figure 2 in ref. 4

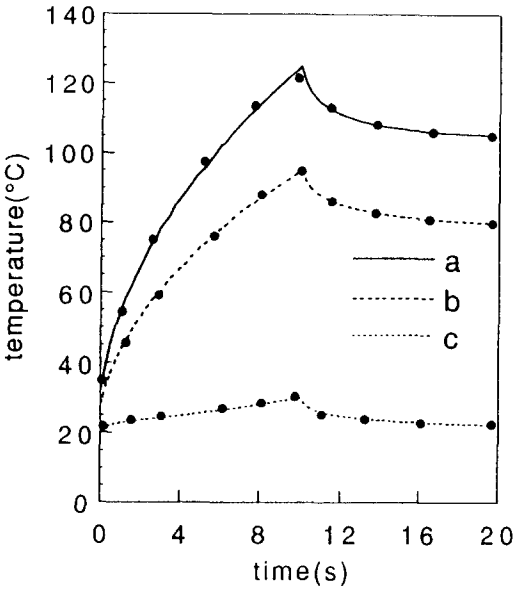

Figure 1 Calculated (lines) and experimental (●) surface temperature *versus* time: (a) $T_r = 1500$ K, $R_i = 20\,000$ W m^{-2}; (b) $T_r = 2000$ K, $R_i = 20\,000$ W m^{-2}; (c) $T_r = 1500$ K, $R_i = 6500$ W m^{-2}

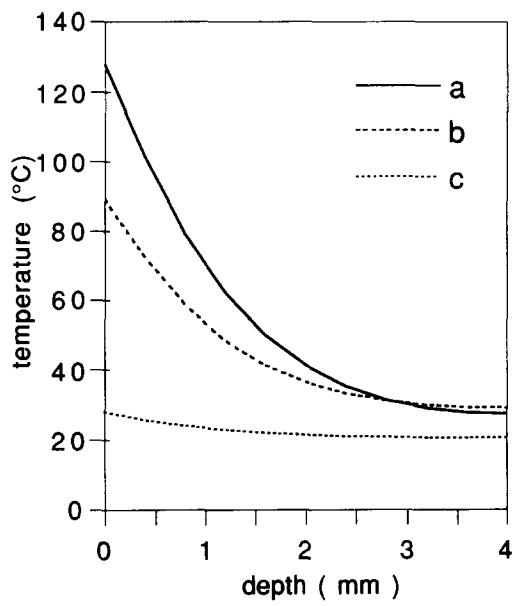

Figure 2 Temperature profile *versus* depth: curves as in *Figure 1*

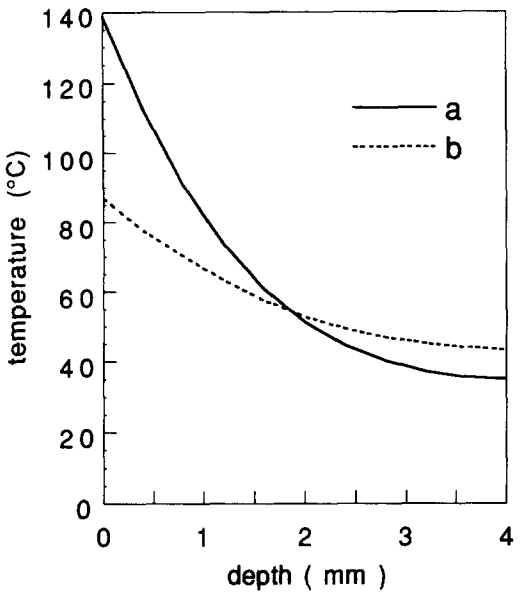

Figure 3 Temperature profile *versus* depth for $T_r = 2000$ K: (a) crystalline; (b) amorphous

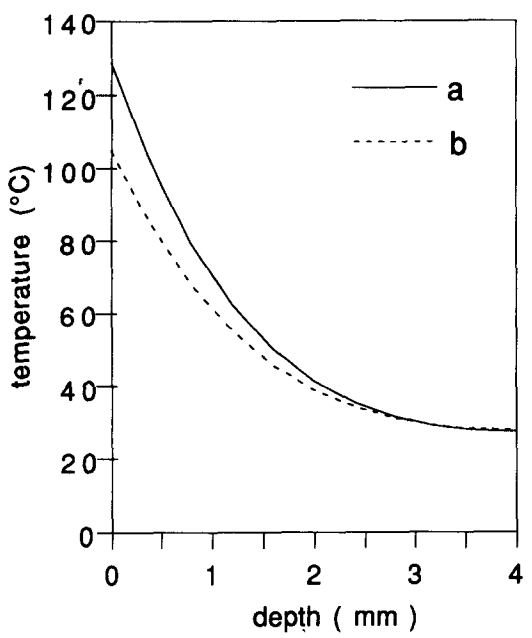

Figure 4 As in *Figure 3*, $T_r = 1500$ K

However, for a semicrystalline polymer, the crystalline structure in the amorphous matrix induces light scattering[9,10] which modifies the penetration depth of the short i.r. waves. Consequently, the radiation heat transfer inside the plate changes when the polymer is crystallized. *Figure 3* shows, in a significant way, the necessity of taking this phenomenon into account (curve a: crystalline, curve b: amorphous). Because of the influence of the skin absorption of the i.r. radiation on the temperature profile, uniform and rapid heating cannot be achieved. On the contrary, if we use long-wave i.r. radiation (radiator temperature = 1500 K) the radiation absorption occurs essentially on the sheet surfaces whatever the material structure (*Figure 4*). Therefore, in this case, the change of optical properties induced by the scattering does not modify drastically the radiative heat transfer and could be neglected (Figure 6 in ref. 4).

Applications of the simulation calculation

In addition to the study of the influence of the material optical properties on the temperature profiles, we will see that the simulation calculation gives an indication about the convective phenomenon and the crystallinity kinetics. Finally, we present an example of optimization of an industrial process.

Influence of convection. The following computational example (*Figure 5*) shows how blowing cooled air ($T_0 = 20$°C) on the front surface during heating influences the temperature profiles advantageously. Without the air jet ($C_0 = 0$ W m^{-2} K^{-1}), the temperature of the front of the plate may exceed the melting temperature (*Figure 5*, curve a). We could avoid this difficulty by reducing the radiation intensity (curve b); however, this reduction implies an increase of the heating time. On the contrary, if the front of the plate is cooled by the air jet ($C_0 = 150$ W m^{-2} K^{-1}), the temperature profiles are advantageously influenced (curve c), and it is then possible to maintain the same radiation intensity and therefore to reduce the heating time. Generally, the increase of the surface cooling improves the temperature uniformity through the sheet but decreases the overall rate of heating (*Figure 5*, curves a and c). This is one of the main problems in polymer processing because two contradictory objectives must be achieved: (1) a high degree of temperature uniformity across the wall thickness and (2) a short heat-up time for efficient production.

Influence of crystallinity. As the stretching temperature range falls between the glass transition temperature and the crystallization temperature, knowledge of the crystallinity is very important. Indeed, the gas permeation through the polymer, the mechanical properties and the transparency depend on the crystallinity value of the semicrystalline polymer. The same holds true for the ability to support temperature above the glass transition

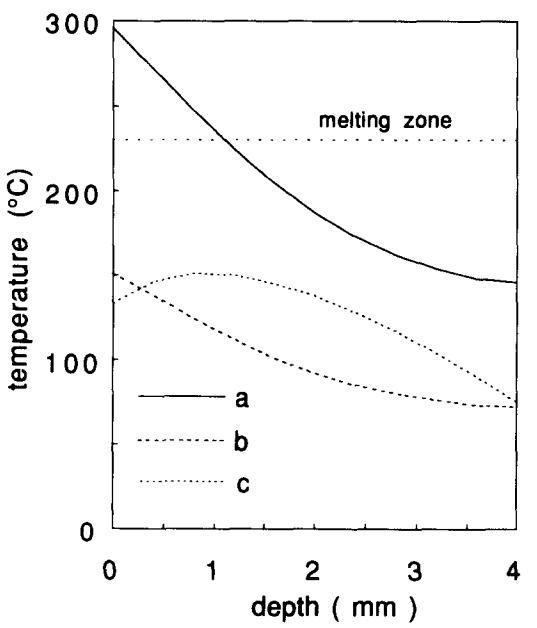

Figure 5 Temperature profile *versus* depth: (a) $C_0 = 0$ W m^{-2} K^{-1}, $R_i = 20\,000$ W m^{-2}; (b) $C_0 = 0$ W m^{-2} K^{-1}, $T_0 = 20$°C, $R_i = 10\,000$ W m^{-2}; (c) $C_0 = 150$ W m^{-2} K^{-1}, $T_0 = 20$°C, $R_i = 20\,000$ W m^{-2}

temperature without any deformation. For these reasons, it is interesting to compare experimental and simulated values of the crystalline distribution inside the material.

The distribution simulation uses the Ozawa[11] theory in which the computed transformed fraction α at the temperature T_p is obtained by[12]:

$$\alpha(T_p) = 1 - \exp - \left[\sum_{i=1}^{p} \left| \frac{\chi^{1/n}(T_i) - \chi^{1/n}(T_{i-1})}{v_i} \right| \right]^n$$

$\chi(T)$, the heating (or cooling) crystallization function of the polymer, and the Avrami number n were determined by means of thermal analysis. The crystallization fraction $X_c(T_p)$, calculated from the value of the transformed volume fraction, is, following Deterre[13], never higher than 40% for PET. The value of this crystallization fraction is obtained by:

$$X_c(T_p)(\%) = 40 \times \alpha(T_p)$$

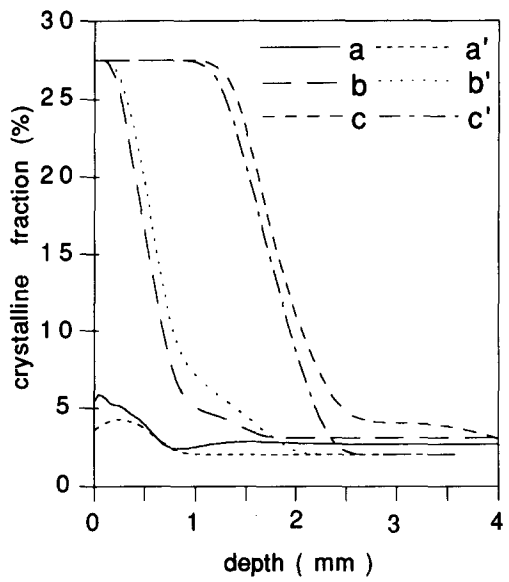

Figure 6 Crystalline fraction distribution *versus* depth for different heating times: (a), (b), (c) experimental results; (a'), (b'), (c') calculated data

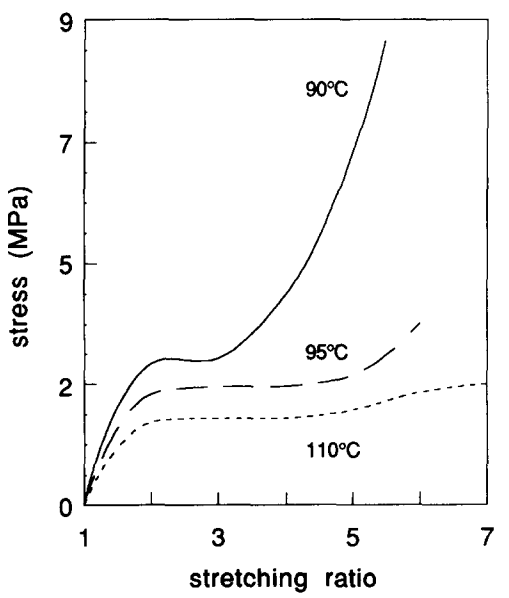

Figure 7 Stress *versus* stretching ratio for different temperatures

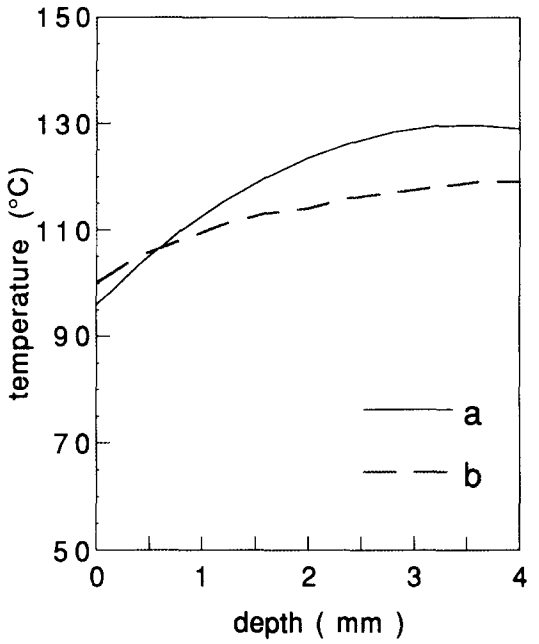

Figure 8 Temperature profile *versus* depth: (a) end of heating; (b) after a 3 s transient time

The experimental crystalline distribution profiles were obtained as follows. First, the front side of 4 mm thick PET plates were heated in the prototype oven with radiators at a temperature of 2400 K for different durations. Next, each heated plate was sectioned using a microtome to obtain slices of 10 μm in thickness and finally the crystalline fraction of the slices was determined by thermal analysis.

The experimental curves are given in *Figure 6* (curves a, b, c) along with the calculated curves (a', b', c') corresponding to the same heating times. We observe a good agreement that allows us to use this model for the determination of the crystalline profile inside a semicrystalline polymer undergoing heat treatment.

Influence of temperature profile on stretching. For special purposes (such as biaxial stretch blow moulding of bottles), non-uniform temperature profiles are induced deliberately throughout the material. Indeed, in this process the front and back stretching ratios λ differ by more than 50% during stretching ($\lambda = 4$ to 6.5). *Figure 7* shows the mechanical behaviour of amorphous polyester at different temperatures. For a given temperature the actual stress is higher on the back than on the front. As uniformity of stress is required, a good stretching process is obtained by deliberately inducing a non-uniform temperature profile into the material. *Figure 8* shows a temperature profile that ensures a good stretching process. These temperature profiles are reached after a 20 s heating time (*Figure 8*, curve a) and a 3 s transient time (curve b).

CONCLUSIONS

The four-flux model in addition with the Ozawa model enables the prediction of temperature, temperature distribution and crystalline profile in PET plates. The differences between experiment and modelling arise essentially from the inability to determine accurately

the thermal parameter values and particularly the convective parameters. Nevertheless, this model is useful for understanding the heating stage of thermoplastic products and it is a suitable tool for the control and optimization of an industrial process.

REFERENCES

1 Cardon, R. *J. Am. Ceram. Soc.* 1958, **41**, 200
2 Esser, K., Haberstroh, E., Hüsgen, U. and Weinand, D. *Adv. Polym. Technol.* 1987, **7**, 89
3 Progelhof, R. C., Quintiere, J. and Throne, J.L. *J. Appl. Polym. Sci.* 1973, **17**, 1227
4 Lebaudy, Ph., Saiter, J. M., Grenet, J. and Vautier, C. *Polymer* 1992, **33**, 1887
5 Maheu, B., Letoulouzan, N. and Gouesbet, G. *Appl. Opt.* 1984, **23**, 3353
6 Dangoux, R., Bissieux, C. and Egee, M. 'Thermal Transfer in Composite Materials', Eurotherm 4, Nancy, 1988
7 de Daubeny, R. P., Bunn, C. W. and Brown, J. *Proc. R. Soc., Ser. A* 1955, **226**, 531
8 Boukined, M. *Thesis*, Université de Rouen, 1992
9 Tabar, R. J., Leite-James, P. and Stein, R. S. *J. Polym. Sci., Polym. Phys. Edn* 1985, **23**, 2085
10 Haudin, J. M. 'Optical Properties of Polymers', Elsevier Applied Science Publishers, New York, 1986
11 Ozawa, T. *Polymer* 1971, **12**, 150
12 Billon, N. *Thesis*, Ecole des Mines, Paris, 1987
13 Deterre, R. *Thesis*, Strasbourg, 1984